

A RISK BASED, MULTI-COMPONENT MODEL TO IDENTIFY CONTAMINANT LOADINGS AND TRANSPORT THROUGH GROUNDWATER SYSTEMS UNDER UNCERTAINTY

TODD A. WANG

U.S. Army, Ft. Bragg, North Carolina

WILLIAM F. McTERNAN

Oklahoma State University, Stillwater

ABSTRACT

We developed and applied a suite of risk-based methods for characterizing the contaminant potentials from a former munitions plant in East Texas. The site was originally “clean closed” when a subsequent groundwater monitoring program disclosed areas of contamination by the chlorinated solvent, trichloroethylene (TCE) and others. As part of an overall decision model developed for the site, a series of probability-based mathematical and statistical models were developed to address off-site contamination and plume configuration. As with most historic hazardous waste sites, there was virtually no information relative to contaminant loading rates to the water table aquifer. These loads were reconstructed by comparing the results generated from a Monte Carlo-based technique which linked the vadose and saturated zone models to minimal groundwater data previously collected. The contaminant flux in the aquifer was assumed to coincide with activities at the munitions plants peaking as the plant was decommissioned and tailing off through subsequent years. This curve followed the classic boundary condition where the contaminant source is terminated after a period of flux into the aquifer. Comparisons between simulated data and the site activity curve indicated that the peak of the contamination had occurred before the monitoring program was initiated, generally matching concentrations along the recession limb. Probabilistic transport modeling through the water table aquifer produced a series of statistical distributions of off-site contamination. These curves further corroborated the observation that peak contamination at this site had occurred before the monitoring data were collected. A Bayesian updating technique was applied to compare the revised probabilities associated with various management alternatives and a conditional simulation was completed to define the plume configuration with some statistical confidence.

INTRODUCTION

Previous work by the authors has been concerned with the development and application of Decision Analysis Models (DAM) which generated alternatives for the remediation of contaminated soil and groundwater at an abandoned munitions manufacturing facility [1, 2]. This article develops and applies the mathematical and geostatistical models employed to identify the contaminant loadings and the transport to and through aquifer systems used in those decision models.

The conditions encountered included minimal available monitoring data to describe either the magnitude or timing of the contaminant loading events through the vadose zone and into and through the water table aquifer. Conditions of this type are frequently encountered when abandoned hazardous waste sites are modeled in conjunction with risk assessments or in advance of remediation design. The approaches evaluated in the subject research can individually address select elements of these uncertainties. The combination of different methods works to better identify multiple sources of possible error.

When used within an overall risk assessment or remediation design sequence, these methods can illuminate areas where additional data collection would be useful while also suggesting alternative approaches for final design or mitigation, including making the case for monitored natural attenuation where appropriate [3].

GENERAL BACKGROUND

In spite of an extensive data collection program initiated by the U.S. Corps of Engineers at this location, the Longhorn Army Ammunition Plant (LHAAP) in east Texas, insufficient and often inappropriate information was available to describe contaminant loading to and movement through the receiving aquifer. Mathematical groundwater transport models with a Monte Carlo simulator were employed to ascertain:

1. the probability of contaminant loads to the receiving aquifer; and
2. the probabilities of occurrence for TCE contamination at an arbitrarily chosen Plain of Compliance (POC).

Conditional simulation was used to establish probability-based spatial estimates of in-place contaminant concentrations to better define plume geometry for risk assessment or remediation purposes. These spatial estimates, together with the attendant probabilities of contaminant occurrence derived from the Monte Carlo transport modeling, were used to help estimate uncertainties associated with the projected chemical concentrations at the POC.

This basic modeling structure was expanded to include Bayesian analyses to compare various alternatives such as the “no action” or monitored natural attenuation alternative, which involved collecting additional monitoring data or

implementing one of three hypothetical remediation approaches. These analyses were predicated on the probabilities of contaminant concentrations at non-detect, below Maximum Contaminant Levels (MCLs) or above MCL levels. These “states of nature” concentrations were initially determined either by applying conditional simulation techniques to existing data or by Monte Carlo-based transport modeling for future conditions. Updating of probabilities by Bayes Theorem integrated these modeling efforts into future remediation decisions undertaken by the design team.

In Bayes Theorem, the prior probability of an event sn_i in the true state of nature is $P[sn_i]$. Revised probability is equal to the conditional probability $[sn_i/Z_j]$ where Z_j is the outcome of a test. The definition of the probability of an intersection and the use of conditional probability definition yields:

$$P[sn_i \cap Z_j] = P[Z_j \cap sn_i] \quad (1)$$

or

$$P[sn_i | Z_j] P[Z_j] = P[Z_j | sn_i] P[sn_i] \quad (2)$$

Rearranging the equation, the posterior probability is obtained.

$$P[sn_i/Z_j] = P[Z_j | sn_i] P[sn_i]/P[Z_j] \quad (3)$$

From equation (3), it can be seen that the revised probability is a function of the prior probability. The sample likelihood $P[Z_j | sn_i]$ is the probability that the test event Z_j occurs given the true conditional state of nature sn_i . Using Bayes Theorem, revised probabilities were determined given the additional information/data that could be gained from newly constructed monitoring wells. Only those potential errors associated with the laboratory analyses of samples from newly constructed, hypothetical wells were considered in this analysis. Bayesian updating relies on identifying the true state of nature given measurable laboratory uncertainties. Other sources of error exist and could be included in the Bayesian updating. The technique employed could be readily expanded to include these additional sources of error should data become available.

SITE DESCRIPTION

Figures 1 and 2 respectively present the geological cross-section information bearing the original munitions plant and the site location in east Texas. The LHAAP is in the middle of the east Texas timber belt, characterized by sandy rolling forested topography [4]. Geological formations beneath the site are the Wilcox and Midway groups [5]. The Wilcox formation in Harrison County is characterized as a depositional facies of tributary channel deposits from the Tertiary age [6].

It is typical for these types of deposits to consist of about 40% channel (sand) and 60% overbank deposits (silt and clay). Due to the depositional environment,

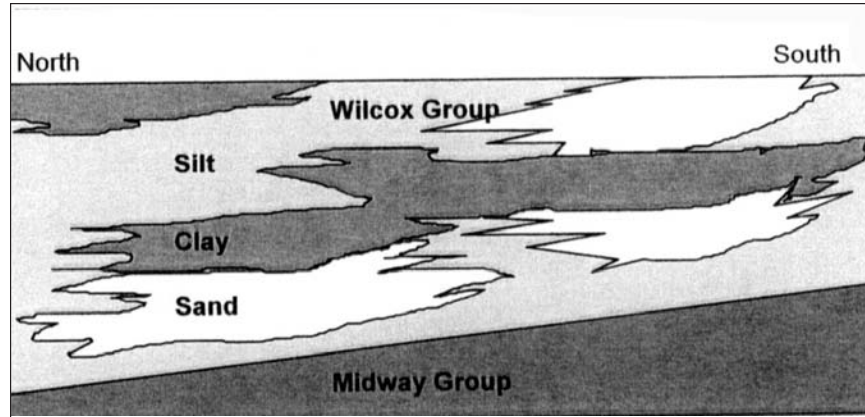


Figure 1. Typical stratigraphic cross section of the Wilcox and Midway groups with detail of interbedded silts, clays and sand (not to scale).

the Wilcox Aquifer is made up of interbedded sand, silt, and clay (Figure 1) [4]. Some clay lenses are extensive enough to cause confining conditions locally [7].

The aquifer varies in depth from 90 to 150 feet, with the Midway group acting as a lower boundary unit. Aquifer depth variance is due to the slight Northwest dipping of the Wilcox and Midway groups caused by the Sabine uplift which has pushed Upper Cretaceous beds to within 700 feet of the surface [8]. In areas adjacent to the uplift the same beds are 5000 to 6000 feet from the surface.

Regional groundwater gradient is about .0015 to the northeast [7], but is affected locally by mounding of the water table beneath the LHAAP. The mounding causes a radial gradient outward from the site for a short distance [9]. This mounding was attributed to the increased levels of infiltration due to activities at the site which removed topsoil and vegetation.

While the capacity of the Wilcox aquifer is small to moderate, its potential use as a domestic water source is high for rural home sites [7]. In addition, the industrial complex is bounded to the Northeast by Caddo Lake that serves as a drinking water source to the local communities of approximately 50,000 people [10]. Therefore, the potential for drinking water contamination from the site exists. With the regional groundwater gradient generally oriented northward, Harrison Bayou, downgradient from the site was categorized as the critical receptor path for transported contaminants and a plain of compliance within the Bayou was established to identify potential receptors to the contaminant of concern. Any contamination migrating beyond the POC with a strength greater than or equal to the set MCL was considered failure. Transport and geostatistical models were used to define the probabilities of contamination existing at this POC. Trichloroethylene (TCE) was used as the chemical marker for these modeling

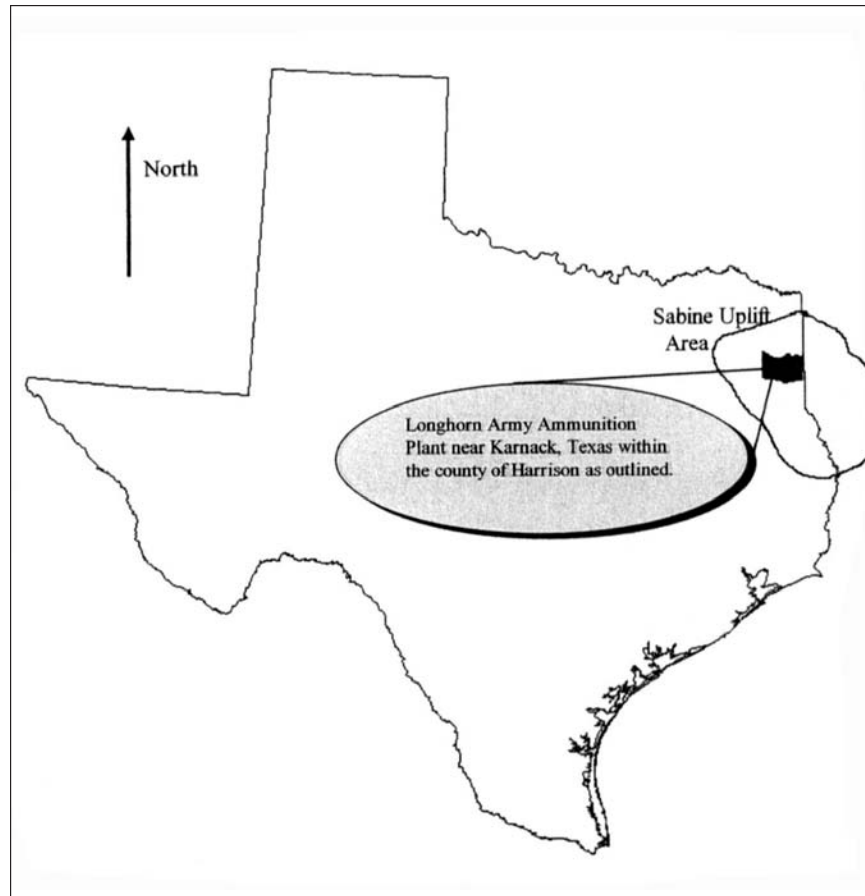


Figure 2. Location of example problem.

efforts because it was identified as a critical contaminant [9]. Other chemicals, however, could also have been used in this effort.

METHODOLOGY

Contaminant Flux to Groundwater Analysis

As is often the case, no information describing contaminant loading from the residuals remaining following clean closure was available. In contrast to cases of pollution of surface waters, particularly point source pollution, leakage from the contaminated vadose zone into a receiving aquifer is neither documented nor

measured. Correct determination of this value, however, is critically important, as it is the basis for all subsequent estimates of groundwater contamination. Typically the analyst employs relatively simple guesses as to the amount of contaminant loading into and through the vadose zone. The guesses are considered “acceptable” if the subsequent simulated contaminant levels in the receiving aquifer are similar to those measured in data collection programs. Many sources of possible error can affect these estimates.

Better, more scientifically-based approaches are needed to estimate the contaminant loading into the aquifer from the vadose zone. The alternative that was developed in this effort used measured data and fundamental transport theory to develop a contaminant loading curve.

Figure 3 presents two theoretical vadose zone contaminant loading curves which could occur for initial and boundary conditions similar to the removal of a contaminant source following an extended period of leakage into and through the vadose zone. Monitoring programs together with a careful examination of production records have indicated that this is the probable mechanism of contamination at the LHAAP [9].

The increase in concentration (or mass loading), as seen between points a and b of curve A, represents the plume’s arrival at a stationary monitoring point. Flattening of the curve, as shown between points b and c, shows plume strength at its maximum indicating continuous loading from the source. Between points c and d the decreasing concentration results from removal or dissolution of the source. Curves A and B represent either alternative compounds with different transport

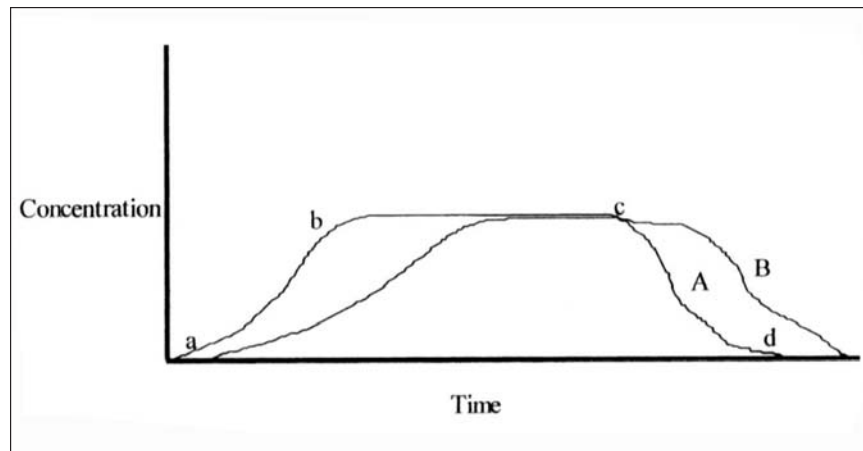


Figure 3. Concentration versus time under alternative, hypothetical advective transport conditions.

properties such as adsorption and/or ion exchange (retardation) or alternative hydrogeological conditions.

Previously measured contaminant soil concentrations and soil properties were used to develop a mass loading curve similar to Figure 3 [9]. As the source was removed in 1985 and was no longer loading TCE into the unsaturated zone, the mass loading to groundwater should lie somewhere between points c and d of Figure 3 and was approximated by advective-dispersive modeling in a two phased effort. The first phase traced mass loading from the time the units were opened (1950) and continued into the mid-1980s with closure in 1985 [4]. As soil contaminant concentrations were not available prior to 1988, the earliest representative soil level was utilized and the following assumptions were made with respect to both modeling phases:

- Phase one thickness of contaminant incorporation was one meter. This was based on the information from the data summary report on depths of the Unlined Evaporation Pond (UEP) and disposal trenches [9].
- For modeling purposes, the depth of the unsaturated zone was considered uniform over the entire site. This figure was derived using simple statistics of the depth to water table data from 44 groundwater wells.
- It is assumed that by 1988 the entire unsaturated zone thickness was contaminated under the source. Therefore, phase two thickness of contaminant incorporation was 5.74 m, equal to the unsaturated zone depth.
- Since the majority of the waste was disposed into trenches and the UEP, it was valid to assume there was no cover over these units [9].
- Fifteen different waste units were located with a area 159 m by 305 m. Since the waste units occupied more than 50% of this area, the area was modeled as a single unit.

A simple statistical analysis of the soil concentration data from 1988 provided a mean and upper boundary of the 95% confidence interval (UB 95 CI) to be used as the contaminant concentration in the soil.

Phase two used the contaminant soil concentration data from 1988 to determine where mass load for that and subsequent years were located on the theoretical curve. From this point, contaminant loading was extrapolated to determine a maximum mass loading into the aquifer.

Tool Used

The Jury unsaturated zone model incorporated in the American Petroleum Institute's Decision Support System for Exposure and Risk Assessment (APIDSS) software was used to estimate the contaminant flux into the aquifer [11, 12]. This model is based on the analytical solution to the differential mass balance equation with appropriate boundary and initial conditions:

Differential mass balance equation:

$$(\partial C_T / \partial t) + \mu C_T = D_E (\partial^2 C_T / \partial z^2) - V_E (\partial C_T / \partial z) \quad (4)$$

where

- C_T = total soil concentration (mg of contamination/cm³ of wet soil)
- t = time (day)
- μ = first order decay rate constant (1/day)
- D_E = effective diffusion coefficient (cm²/d)
- z = depth measured positive downwards from the soil surface (cm)
- V_E = effective contaminant velocity (cm/d)

The initial condition is:

$$C_T(0 < z < L, t = 0) = C_o \quad (4a)$$

$$C_T(z \geq L, t = 0) = 0 \quad (4b)$$

Equations (4a) and (4b) imply that initially the contaminant is uniformly incorporated to a depth L. In equation (4), the total soil concentration is assumed to be distributed between the solid, aqueous, and vapor phases. Concentrations estimated at the water table are used to compute the contaminant flux to the water table using:

$$M_{wt} = VC_1A + D(\Delta C / \Delta Z)A \quad (5)$$

where

- M_{wt} = annual mass loading to water table (mg/yr)
- V = infiltration rate (m/yr)
- A = area of the source (m²)
- C_1 = liquid phase concentration at the water table (mg/m³)
- D = hydrodynamic dispersion coefficient (m²/yr)
- $\Delta C / \Delta Z$ = concentration gradient at the water table (mg/m³/m)

From the modeling analysis, the estimated peak mass loading occurred in year 24 or calendar year 1974. Year 0 corresponded to calendar year 1950, when contaminant disposal started. Maximum loading was maintained for a period of 11 years, from 1974 to 1985. In 1985 the site was closed with removal of all solids and liquids [4]. This period was used to construct the b-c equivalent segment of Figure 3 with the simulated mass loading data. The resultant curve was then used to determine the pulse load (yearly loading into the aquifer) by graphical integration. Two soil concentrations were employed: the mean and the UB 95 CI.

Transport to Plain of Compliance (POC)

Following the development of this source-loading curve, a second contaminant transport activity was initiated to determine the probability of the plume reaching the POC at a specified concentration. A publicly available two-dimensional analytical model with a Monte Carlo simulation was utilized to develop numerous possible scenarios [11, 13]. Numerous concentration break-through curves, generated to show the time and concentration relationship of TCE at the POC, were statistically analyzed and cumulative probability density plots developed.

The probabilities developed were utilized within the decision analysis model to assign probabilities for the previously introduced states of nature. Uncertainty of contaminant transport is quantified as a probability that can be integrated into the decision analysis.

Tool Used

Analytical Transport: One, Two and Three Dimensional (AT123D), in the APIDSS software package was used for this analysis [11]. The code, developed by G. T. Yeh in 1981 at the Oak Ridge National Laboratory, Oak Ridge, Tennessee uses Green's function to solve the advection-dispersion transport equation for a variety of source and boundary conditions [13].

Pertinent equations governing the transport and distribution of soluble contaminant are:

$$\frac{\partial n_e C}{\partial t} = \nabla(n_e D \nabla C) - \nabla(C \mathbf{q}) + M - (K n_e C) - (\lambda n_e C) - \frac{\partial(\rho_b C_s)}{\partial t} + (\lambda \rho_b C_s) \quad (6)$$

where

- \mathbf{q} = Darcy velocity vector (L/T)
- D = hydraulic dispersion coefficient tensor (L²/T)
- C = dissolved concentration of the solute (M/L³)
- C_s = absorbed concentration in the solid (M/M)
- ρ_b = bulk density of the media (M/L³)
- M = rate of release of source (M/(L³*T))
- n_e = effective porosity (L^o)
- λ = radioactive decay constant (1/T)
- K = degradation rate (1/T)

This fundamental advective-dispersion solute transport equation in three-dimensions can be simplified if the following assumptions are made:

- Groundwater characteristics are considered uniform. Because the transport of TCE is primarily through highly conductive channel sand deposits within the Wilcox aquifer, modeling the transport within a finite aquifer (channel sand deposits) which can be assumed homogeneous.

- Sorption can be described with an instantaneous linear isothermal equilibrium.
- No waste flow exists across impervious boundaries.
- Flow through open boundaries occurs at infinity.
- There is a finite duration for contaminant release.

Solution of equation (4) is reduced to:

$$C(x,y,z,t) = \int_0^T [M/(n_e R_d)] F_{ijk}(x,y,z,t;\tau) d\tau \quad (7)$$

where

F_{ijk} = integral of Green's function over the source space

M = instantaneous release of total mass

T = duration of waste release

CONTAMINANT PLUME UNCERTAINTY

Geostatistic Applications

This analysis used geostatistical techniques to develop an isoconcentration map of the TCE plume. Even though there were 40 sampling points within the site, there was still uncertainty with respect to the plume's dimensions and concentration contours. The output from this analysis was important to the decision analysis because the plume characteristics were used to identify alternative remedial actions and their attendant costs for the subsequent decision model.

Method Developed and Applied

The flow chart in Figure 4 shows the geostatistical methods used. Following data collection from the sample sites, variance analysis was conducted to determine the spatial statistics among the sampling points. Experimental and modeled semivariograms were developed to describe the pattern of spatial correlation displayed by the data [14-16].

The sample data declustering step was used for this data set because many of the sample points were close to one another. Clustering of wells within the plume is common for groundwater contamination problems because the objective is to locate and define the plume. The collected data may be skewed, and may not truly represent the entire area of concern. To obtain a representative distribution, one can assign declustering weights, whereby values in areas with more data receive less weight than those in sparsely sampled areas [17].

Conditional simulation was used to estimate the concentration of the contaminant at unsampled locations. This Monte Carlo technique generates multiple random realizations of two- or three-dimensional fields of a regionalized variable

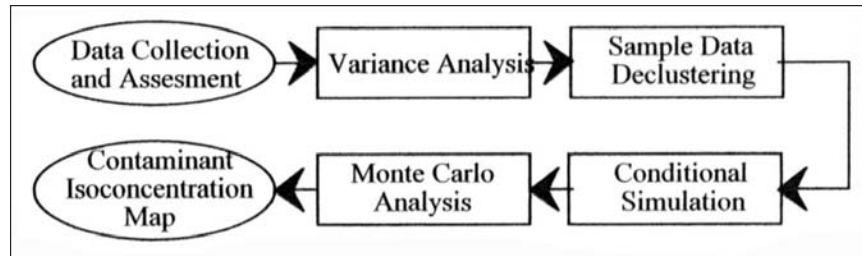


Figure 4. Applicable geostatistical methods employed.

[18]. A simulation is considered conditioned when it honors the observed values of the regionalized variable [19]. A conditional simulation can thus be defined as a surface which has the same variability as the studied phenomenon and which passes through the observed points maintaining their values [20]. When many simulations are completed, the statistical distribution of the contaminant concentrations can be assessed [18]. This analysis results in an isoconcentration map for the TCE plume and a measure of statistical variance around each point that can be used within the decision model.

Methods Applied

Goovaerts [15] and ASCE [21] discuss calculation of the experimental variogram and fitting a model to the variogram. Two moments of $Z(x)$ (with $Z(x)$ representing the random function of contaminant densities) are required for a linear geostatistical analysis. The first-order moment is the mean of $Z(x)$ and the second-order moment includes:

$$\text{variance: } \text{Var}[Z(x)] = E\{[Z(x) - m]^2\} = C(0) \quad (8)$$

$$\text{covariance: } C(\mathbf{h}) = E\{[Z(x + \mathbf{h})][Z(x)]\} - m^2 \quad (9)$$

$$\text{variogram: } 2\gamma(\mathbf{h}) = E\{[Z(x + \mathbf{h}) - Z(x)]^2\} = C(0) - C(\mathbf{h}) \quad (10)$$

where

m = $E[Z(x)]$ = mean or expected value

\mathbf{h} = $x_i - x_{i+1}$ (vector)

$\gamma(\mathbf{h})$ = variogram in the form used most often

The semivariogram is the principal tool used in geostatistics because it can be applied with less restrictive assumptions than either the variance or covariance [14]. The true semivariogram, called the experimental semivariogram, is unknown and is estimated by:

$$\gamma^*(\mathbf{h}) = [2N(\mathbf{h})]^{-1} \sum_{i=1}^{N(\mathbf{h})} [z(x_{i+\mathbf{h}}) - z(x_i)]^2 \quad (11)$$

where

$N(\mathbf{h})$ = the number of sample pairs separated by the vector \mathbf{h} .

The semivariograms generated together with the sampled data were used in the conditional simulation (CS) to generate two-dimensional realizations of the regionalized variable (log-normal TCE concentration). The idea is to develop an isoconcentration map of the plume within some designated confidence interval.

Tool Used

The sequential Gaussian simulation program (SGSIM) was utilized for the conditional simulation step [22]. This algorithm produces directly conditioned estimates without an intermediate unconditioned step. Sequential simulation conditioning is extended to include all data available within a neighborhood of the simulated variable, including the original data and all previously simulated values.

With SGSIM, each variable was simulated sequentially according to its normal conditional cumulative distribution function (ccdf), fully characterized through a simple kriging system [22]. The conditioning data consist of all original data and all previously simulated values found within a neighborhood of the location being simulated.

With this approach the conditional simulation of a continuous variable $z(\mathbf{u})$ modeled by a Gaussian-related stationary random function $Z(\mathbf{u})$ proceeds:

- Using the cumulative distribution function (cdf) $F_z(z)$, performs the normal score transform of z -data into y -data with a standard normal cumulative distribution function.
- Defines a random path that visits each node of the grid (not necessarily regular) once. At each node \mathbf{u} , retains a specified number of neighboring conditioning data including both original y -data and previously simulated grid node y -values.
- Uses simple kriging with the normal score variogram model to determine the parameters (mean and variance) of the ccdf of the random function $Y(\mathbf{u})$ at location \mathbf{u} .
- Draws a simulated value $y^{(l)}(\mathbf{u})$ from the ccdf.
- Adds the simulated value $y^{(l)}(\mathbf{u})$ to the data set.
- Proceeds to the next node, and loop until all nodes are simulated.
- Back-transforms the simulated normal values $\{y^{(l)}(\mathbf{u}), \mathbf{u} \in A\}$ into simulated values for the original variable $\{z^{(l)}(\mathbf{u}) = \varphi^{-1}(y^{(l)}(\mathbf{u})), \mathbf{u} \in A\}$.
- For multiple realizations $\{z^{(l)}(\mathbf{u}), \mathbf{u} \in A\}, l = 1, \dots, L$, the previous algorithm is repeated L times with either one of the following options: Uses the same random path to visit nodes or a different random path for each realization.

Monte Carlo Analysis

Each of the numerous simulations represents a possible realization of the true TCE concentrations within the groundwater aquifer. A statistical analysis was conducted on the numerous simulations to determine the isoconcentration map of the TCE plume within certain confidence intervals. Three product outcomes were generated: a mean isoconcentration map, an upper boundary of the 95% confidence interval map and an upper boundary of the 90% confidence interval map.

The contaminated site was represented on a grid network of 75 feet square, 3750 feet East-West boundary and 4500 feet North-South boundary. Each grid intersection was represented by a node for which a value $z^{(j)}(\mathbf{u})$ was simulated. A statistical analysis was calculated for each of the node locations to estimate the cumulative probability distribution. If $z(\mathbf{u})$ represents the true concentration value at any node:

$$z(\mathbf{u}) = g(\mathbf{X}) \quad (12)$$

where

g = function representing the conditional simulation

\mathbf{X} = vector of all simulation inputs [23].

Since the components of \mathbf{X} contain the cumulative distribution function (cdf) $F_z(z)$, the goal of Monte Carlo analysis is to calculate the cdf $F_{z(\mathbf{u})}(z_s(\mathbf{u}))$ given the probabilistic characterization of \mathbf{X} [23]. $F_{z(\mathbf{u})}(z_s(\mathbf{u}))$ is defined as:

$$F_{z(\mathbf{u})}(z_s(\mathbf{u})) = \text{Probability}(z(\mathbf{u}) \leq z_s(\mathbf{u})) \quad (13)$$

where

$z_s(\mathbf{u})$ = is the CS output

Given a set of deterministic values for each of the input parameters, X_1, X_2, \dots, X_n , SGSIM computes the output simulation value as:

$$z(\mathbf{u}) = g(X_1, X_2, \dots, X_n) \quad (14)$$

Application of the Monte Carlo simulation procedure requires that at least one of the input variables, X_n , be uncertain and that the uncertainty be represented by a cumulative probability distribution. The simulation is then conducted numerous times to generate a series of $z_s(\mathbf{u})$ values for each of the nodes within the two-dimensional grid simulated [24]. The simulated outputs are then statistically analyzed to yield the cumulative probability distribution of the simulated output. The steps involved in the application of the Monte Carlo technique include:

- Select the appropriate cumulative probability distribution function for describing uncertainty in the input variable(s).
- Select a random number from the distribution and use this as input to the model.

- Run the model using the random number taken from the input distribution to calculate the output.
- Repeat steps 2 and 3 for a number (n) times.
- Determine the cumulative probability distribution function of the output step 3
- Analyze the output distribution and utilize the statistics (i.e., mean and UB 95 CI).

A subsequent grid with the statistical values of the simulated values was developed on a spreadsheet and plotted.

RESULTS

Mass Loading to Vadose Zone

Figure 5 illustrates the first and second phase modeling curves developed by the Jury transport model. First-phase modeling developed the shape of curve A in Figure 5 with respect to the actual time line of events at the LHAAP. The second-phase modeling developed the darkened portion of curve A, between points c and d, and was used to determine mass loading over time. The maximum mass loading, point c, was then extrapolated from phase two modeling values and phase one curve shape. This analysis shows that much of the residual TCE had leached into the aquifer prior to the initiation of soil monitoring programs in 1988.

Figure 6 presents the final calculations of the total TCE loading to the aquifer beginning in 1967, increasing through 1973 and then decreasing from 1985 to 1997 as inplace TCE reached residual saturation. The area under this curve represents the total mass of TCE that was loaded into the aquifer at the mean and higher flux rates. Multiplying the mass loading (kg/yr) by the number of years yielded the mass of TCE in kilograms. Calculation was done for both curves. Total loading values calculated for the UB 95 CI and mean curves were 18,942 kg and 7998 kg, respectively. The total load values were divided by 30 years to derive uniform pulse loadings of 631 kg/yr and 267 kg/yr for the UB 95 CI and mean curves respectively, to be used in the saturated zone transport model.

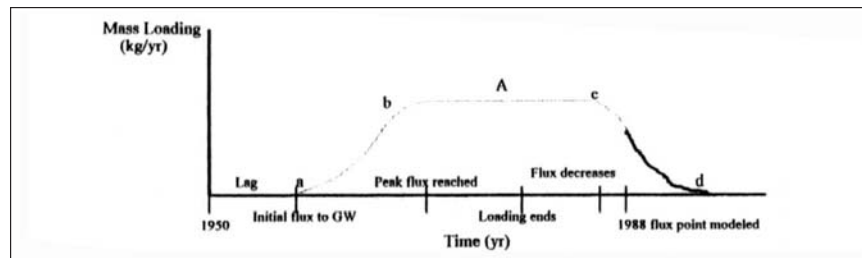


Figure 5. Vadose zone mass loading plot.

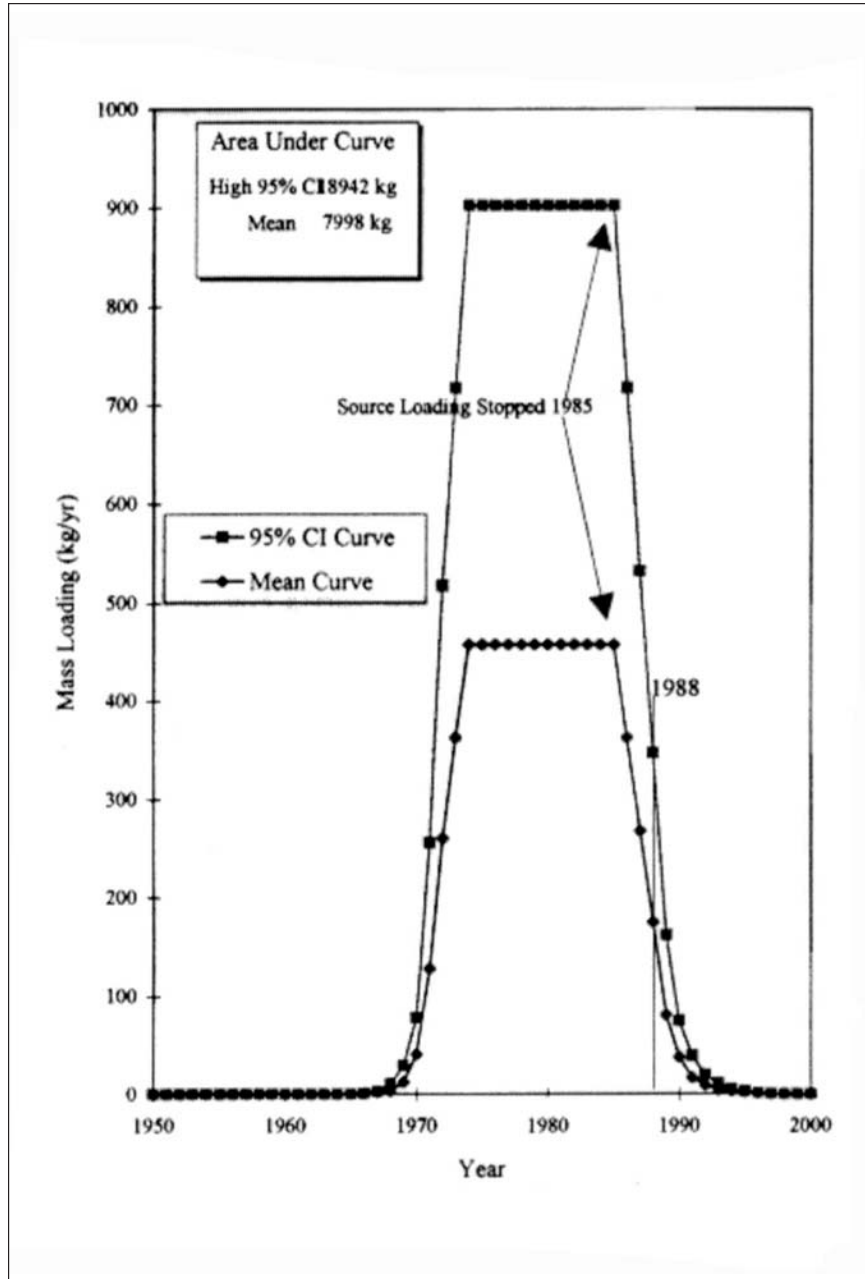


Figure 6. Mass loading of TCE to groundwater at the burning grounds using Jury model.

Transport to Plane of Compliance (POC)

The stochastic groundwater transport modeling effort was tested in two ways to address the validity of the models developed. The first way addressed the adequacy of the Monte Carlo sampling protocol while the second effort compared the modeled data with equivalent data collected during the historical monitoring program.

Maximum Precision Determination

The method used to determine the maximum precision of the Monte Carlo analysis plotted the mean concentration at the receptor point (POC) against the number of simulations. As the number of simulations increased, the mean concentrations oscillated around a maximum precision value. When the analysis produced a relatively constant result, maximum precision was achieved.

Figure 7 shows that maximum precision of the Monte Carlo analysis occurred between 275 and 300 simulations. Mean concentrations from 1 through 100 simulations showed much variation before tapering to a relatively constant point which occurred at about 250 simulations with a mean concentration of .0015 mg/l (1.5 ug/l). The 300 simulations used in this analysis were beyond the minimum required simulations for maximum precision. Simulation numbers beyond 300 theoretically have no effect on the stochastic analysis.

Model Calibration

As a check to ensure that the contaminant transport simulations were producing reasonable results, a calibration analysis was made. During this analysis, all model parameters were held constant with transport to an adjacent monitoring well replacing the simulations to the POC. The monitoring well chosen had consistent hydrologic connection with the original contaminated source and an extensive monitoring history spanning 11 years (1982-1993) [9]. Geologic cross-sections showed a channel sand deposit connecting the well with the UEP [9]. This provided the best possible homogeneous situation in which to conduct the simulations. No TCE contamination was detected during initial monitoring efforts of 1982. In subsequent years, however, the detected amounts fluctuated between 29 and 10,000 ug/l.

The results of these calibration efforts are presented in Table 1 which compares the measured data from the monitoring well for years 1982-1993 to the modeled concentrations. The comparisons in Table 1 show that the modeled TCE concentrations approximated the measured ranges. Years 1986-1992 had a higher measured concentration than the model predicted but were within the same order of magnitude. Results of this analysis illustrate some reliability in the modeling parameters used in modeling contaminant transport.

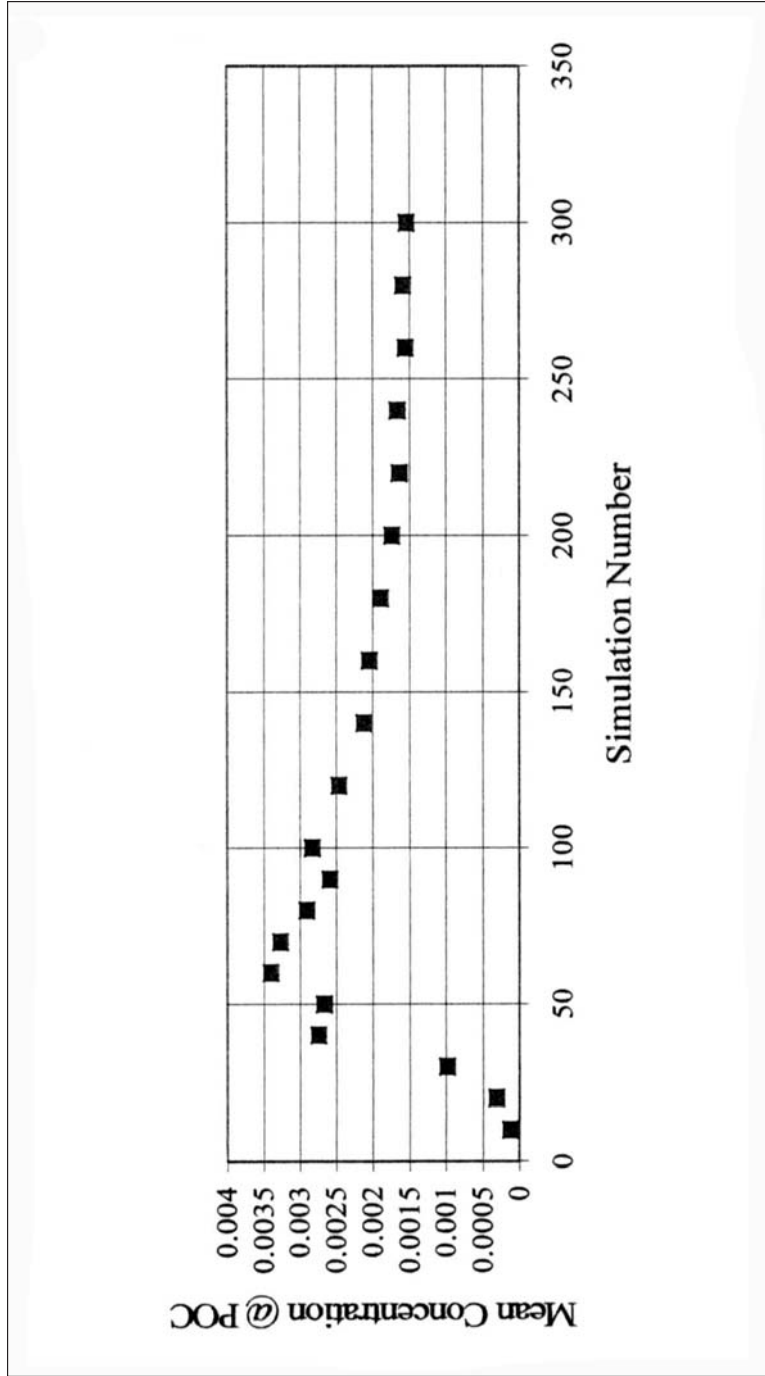


Figure 7. Maximum precision plot for Monte Carlo analysis.

Table 1. Comparison of Monitoring to Modeling Data

Year measured/simulated	Measuring data (mg/l)	Modeling data (range in mg/l)
NOV 82/year 32	not detected	0-.09
APR 83/year 33	.029	0-.09
SEP 84/year 34	<.05	0-.09
SEP 86/year 36	.11	0-.09
SEP 87/year 37	.16	0-.09
SEP 88/year 38	.19	0-.10
NOV 92/year 42	.204	0-.02
NOV 93/year 43	.094	0-.01

Contaminant Transport Probabilities

These Monte Carlo simulations were statistically analyzed to form a probability distribution plot for TCE concentrations at the POC for various time periods. Figure 8 illustrates an example of a probability plot for five time periods. In Figure 8 each of the five curves illustrated the probability distribution of contamination at the POC within a specific time period. Curve A represents the probability distribution of the simulated TCE concentrations at the POC within the entire 50-year simulation period. Subsequent curves illustrate similar probability distribution of concentrations for different incremental time periods within the 50-year simulation. Curve B shows the probability distribution of simulated concentrations at the POC for simulation years 1-10 as does curve C for simulation years 11-20. Curves B and C show a significant difference in probability distribution. That is, the probability for .001 mg/l (1 ug/l) of a TCE to migrate to the POC is about 19% in the first 10 years, as opposed to 2% in the following 10 years, as represented by curve C. After 20 years, the probability is almost zero, as shown by curves D and E. Probability curves B and C are important factors in analyzing the decision to postpone any remedial actions.

Table 2 presents the results from the Bayesian simulations where prior probability distributions were updated with outputs from the stochastic transport models. It should be noted that these probabilities were developed in conjunction with the previously referenced decision model (not included in this article). These results are included, however, as they further quantify and support those developed by the stochastic transport analyses and serve as a basis for the geostatistical evaluations which follow. These revised probabilities were developed for:

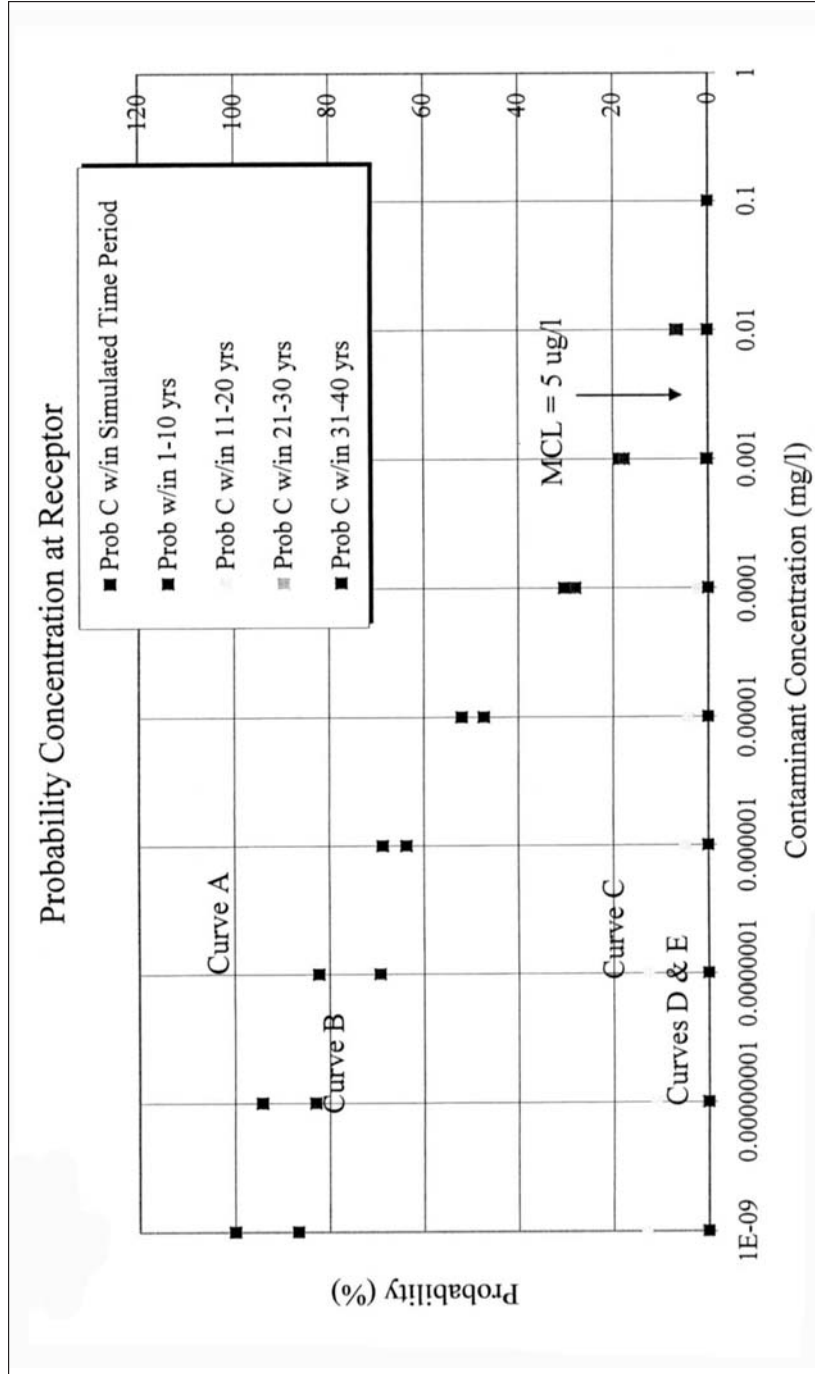


Figure 8. Contaminant transport probability for concentrations at the POC.

Table 2. Revised Probabilities Utilized within the Decision Tree Analysis

Decision tree analysis		Probability (%)		
Decision alternative	Test result	sn ₁	sn ₂	sn ₃
Take action	No additional testing	52	35	13
Additional testing	No detection of contaminant	100	0	0
	Detection < 5 ug/l	46	42	12
	Detection ≥ 5 ug/l	0	67	33
Postpone action 10 yrs	No detection of contaminant	100	0	0
	Detection of < 5 ug/l	95	4.5	.5
	Detection of ≥ 5 ug/l	0	86	14

- Take Action
- Additional Site Testing
- Postpone Action

alternatives. Prior to the transport analysis, the probability for any one state of nature to occur was 33.3%, since the sum of the probabilities must equal 100%. After conducting the contaminant transport modeling, the probabilities were revised to 52%, 35%, and 13% for sn₁, sn₂, and sn₃, respectively, for actions taken within the first 10 years of simulation. However, if **Additional Site Testing** or **Postpone Action** decisions were made, the sn_x probabilities were changed, as summarized in Table 2, such that if remediation action was postponed 10 years there was only a 14% chance that the TCE concentration would exceed 5 ug/l. Additional testing lowers the probability of not detecting the contaminant to zero while producing a 33% chance that it will exceed 5 ug/l.

Contaminant Plume Delineation

Data Spatial Variance Analysis

A nested Gaussian model characterized by a sill of 7.8, a nugget of 0.0, and a range of 425 feet was developed from two experimental variograms fitted to the Corps of Engineers monitoring data to achieve near origin as well as distance estimation of the collected data. These modeled variograms were then employed in the conditional simulation to generate contour maps of alternative probabilities of the TCE contamination. The environmental decision-maker could then choose an acceptable level of certainty for inclusion into the analysis model described in the accompanying paper.

Monte Carlo Maximum Precision

The same technique used in the transport analysis was applied to the stochastic spatial analysis to determine the minimum number of conditional simulations needed. As there were 3000 simulated nodes for each realization, statistically analyzing all the nodes and plotting the results was not feasible. After removing actual testing locations from the database, three randomly selected nodes were used in the analysis, which showed that maximum precision was reached between 40 and 60 simulations at each of the three simulated nodes.

Statistically-derived isoconcentration maps illustrating the upper boundaries of the 90 and 95% confidence intervals as well as the mean concentrations were prepared. The plot of the simulated means (Figure 9) was very similar to the kriged estimate (not presented) illustrating that the average of conditional simulations at a given location converged to the kriging estimate and the variance converges to the kriging variance as required by the theory [18]. This similarity lends itself to the verification of maximum precision and that 45 simulations were adequate to represent the data.

An advantage of conditional simulation is the ability to produce estimates of the spatial variable with greater resolution. Figures 9 and 10 are the mean (50%) and statistical upper bound 95% confidence intervals (e.g., UB 95 CI) plumes respectively. Comparing the mean with the UB95CI plume illustrates the concentration variations or uncertainties associated with identifying the relative plume concentrations and their areal distributions. Comparison of the two figures revealed that while the areal spread of the respective simulated plumes was about the same for each of these estimates, differences occurred in the concentration distributions where higher contaminant concentrations were observed in the UB95 simulation than in the 50% plot. Greater resolution was achieved in the UB 95 CI plume. That may prove significant in determining remediation alternatives and attendant costs based on the size and strength of the contaminant plume or in making soil-based risk assessments. These figures help define the region where remedial efforts need to be addressed. When used in conjunction with the contaminant probabilities at the POC presented in Figure 8 and the updated Bayesian probabilities presented in Table 2, these figures characterize the monitored natural attenuation region within a statistically established criterion. The routinely used “mean” plume can be compared to either the UB 90 or UB 95 for regulatory compliance.

SUMMARY

The research presented applied multicomponent, risk-based approaches to reconstruct an unmeasured contaminant loading event from a documented vadose zone storage into and through a water table aquifer. Probability-based techniques were used to define statistical distributions of contaminants introduced to the

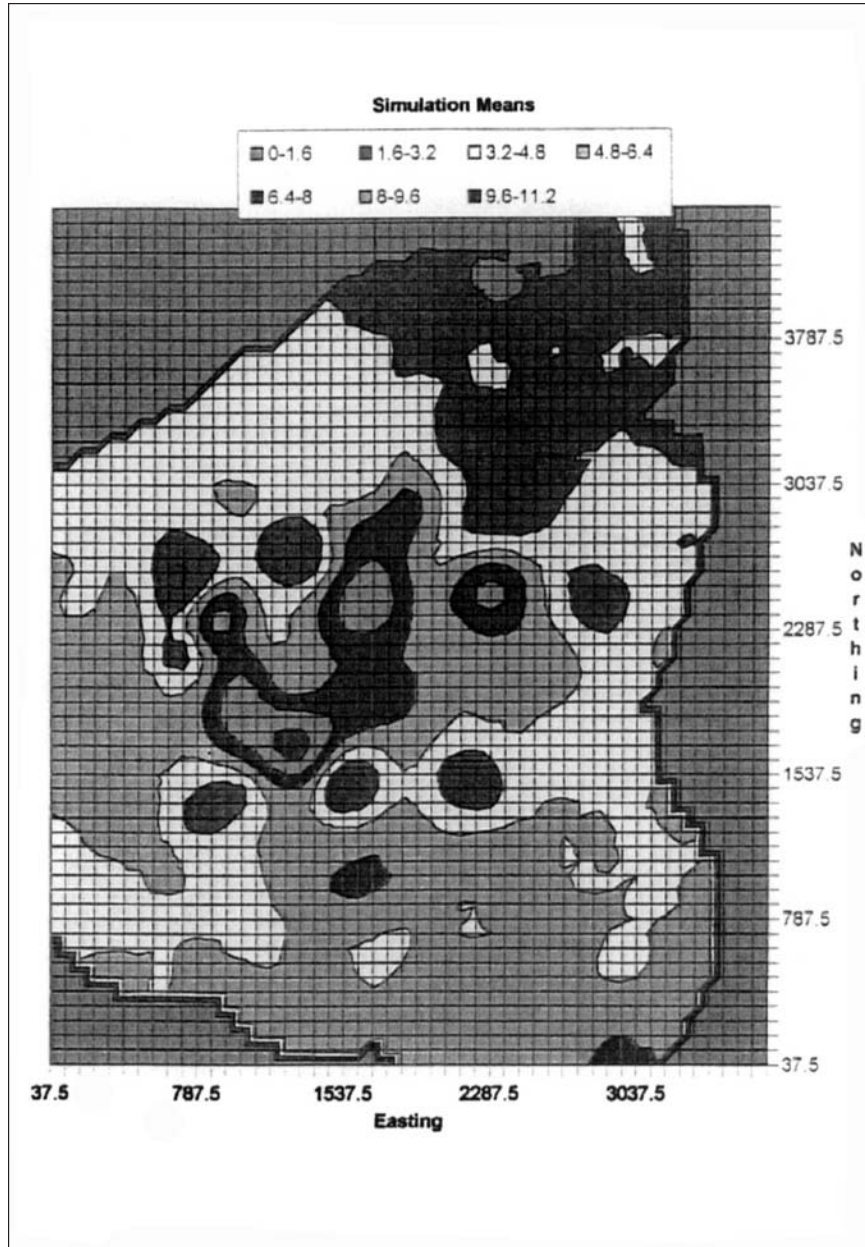


Figure 9. Isoconcentration map of the mean TCE plume from the conditional simulation realizations. The legend gives the TCE concentrations as log-normal transformed.

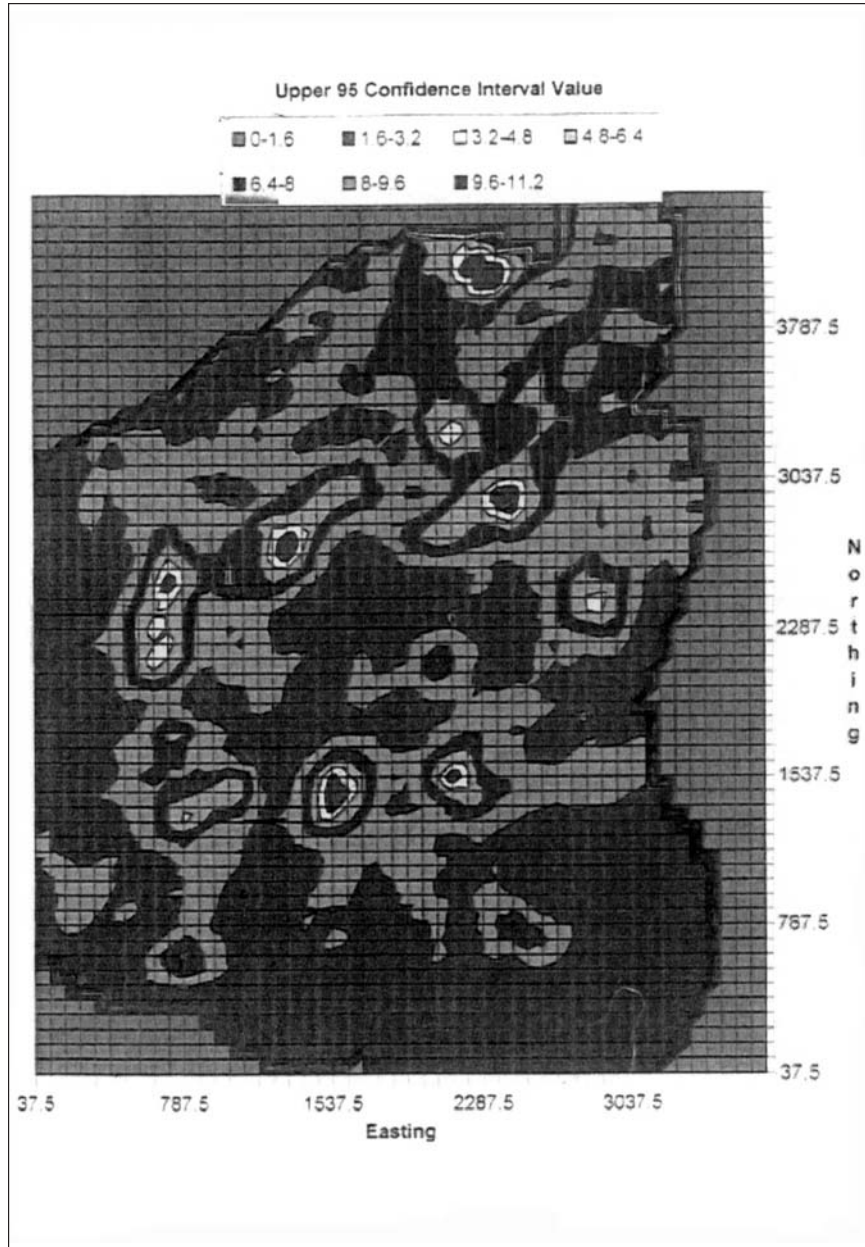


Figure 10. Isoconcentration map of the UB 95 CI from the conditional simulation realizations. The legend gives the TCE concentrations as log-normal transformed.

aquifer and to define chemical concentrations at a down-gradient, off-site location. When these results showed that projected, unacceptable contamination events at this location were relatively infrequent, additional evaluations were undertaken to update these transport probabilities with Bayesian statistics linked to a decision model to further refine risk levels and potential remediation approaches. While the decision model is not covered in this article, as it has been reported previously, these results are included herein since they serve as a starting point in evaluating plume sizes and configurations for possible monitored natural attenuation decisions and additional data collection programs [2]. The areal extent and concentration distribution of the contaminant plume was defined by conditional simulation.

The combination of stochastic transport modeling, Bayesian updating, and geostatistical simulation offers great power in helping determine in a scientifically credible manner which sites should be remediated, over what time intervals, and to what levels. The combined methodology tracked contamination from the vadose zone into the receiving aquifer to points of potential exposure to human and critical ecological receptors. Given the results generated in these analyses, this site appears to be a suitable candidate for remediation based upon natural attenuation.

REFERENCES

1. T. A. Wang, W. F. McTernan, and K. D. Willett, A Risk Based Decision Model to Optimize Remediation Choices at a Superfund Site, in *Superfund Risk Assessment in Soil Contamination Studies, ASTM STP 1338*, D. B. Hodinott (ed.), ASTM, West Conshohocken, Pennsylvania, 1998.
2. T. A. Wang and W. F. McTernan, The Development and Application of a Multilevel Decision Analysis Model for the Remediation of Contaminated Groundwater Under Uncertainty, *Journal of Environmental Management*, 64, pp. 221-235, 2002.
3. F. H. Chapelle, M. A. Widdowson, J. S. Brauner, E. Mendez, and C. C. Casey, Methodology for Estimating Times of Remediation Associated with Monitored Natural Attenuation, *U.S. Geological Survey: Water Resources Investigations Report 03-4057*, Columbia, South Carolina, 2003.
4. M. G. Green and A. J. Marr, Closure of an Unlined Evaporation Pond: A Case History, *Bulletin of the Association of Engineering Geologists*, 27:2, pp. 235-243, 1998.
5. E. M. Cushing, E. H. Boswell, and R. L. Hosman, *General Geology of the Mississippi Embayment*. U.S. Geological Survey Professional Paper 448-B, 1964.
6. W. L. Fisher and J. H. McGowan, Depositional Systems in Wilcox Group (Eocene) of Texas and Their Occurrence of Oil and Gas, *The American Association of Petroleum Geologists Bulletin*, 53:1, pp. 30-54, 1969.
7. R. L. Hosman and J. S. Weiss, Geohydrologic Units of the Mississippi Embayment and Texas Coastal Uplands Aquifer Systems, South-Central United States. U.S. Geological Survey Professional Paper 1416-B, Reston, Virginia, 1991.

8. G. C. Matson, *The Caddo Oil and Gas Field, Louisiana and Texas*, U.S. Geological Survey Bulletin 619, 1916.
9. U.S. Army Corps of Engineers (USACE). *Tulsa, OK District, Data Summary Report of Investigation Results from 1976 through 1992 for Burning Ground 3 and the Unlined Evaporation Pond, Longhorn Army Ammunition Plant, Karnack, Texas*, U.S. Army Corps of Engineers, Tulsa, Oklahoma, 1993.
10. M. L. Golden, A. C. Peer, and S. E. Brown, Jr., *Soil Survey of Harrison County, Texas*. Soil Conservation Service, United States Department of Agriculture, Washington, D.C., 1994.
11. American Petroleum Institute, *Decision Support System for Exposure and Risk Assessment (APIDSS) User Manual* (Version 1.0), American Petroleum Institute, New York, 1994.
12. W. A. Jury, W. F. Spencer, and W. J. Farmer, Behavior Assessment Model for Trace Organics in Soil-1, Model Description, *Journal of Environmental Quality*, 12, pp. 558-564, 1983.
13. G. T. Yeh, AT123D: *Analytical Transient One- Two- and Three-Dimensional Simulation of Waste Transport in the Aquifer System*, Environmental Sciences Division Publication No. 1439, Oak Ridge National Laboratory, Oak Ridge, 1981.
14. R. M. Cooper and J. D. Istok, Geostatistics Applied to Groundwater Contamination. I; Methodology, *Journal of Environmental Engineering*, 114:2, pp. 270-299, 1988.
15. P. Goovaerts, Geostatistical Tools for Characterizing the Spatial Variability of Microbial and Physico-Chemical Soil Properties. *Biology of Fertile Soils*, 27, pp. 315-334, 1998.
16. E. Englund and A. Sparks, *Geostatistical Environmental Assessment Software User's Guide*. U.S. Environmental Protection Agency, EPA 600/8-91/008, Las Vegas, Nevada, 1991.
17. C. V. Deutsch, DECLUS: A FORTRAN 77 Program for Determining Optimum Spatial Declustering Weights, *Computers and Geosciences*, 15:3, pp. 325-332, 1989.
18. J. P. Delhomme, Spatial Variability and Uncertainty in Groundwater Flow Parameters: A Geostatistical Approach, *Water Resources Research*, 15:2, pp. 269-280, 1979.
19. M. E. Hohn, *Geostatistics and Petroleum Geology*, Van Nostrand Reinhold, New York, 1988.
20. J. P. Delhomme, Kriging in the Geosciences, *Advances in Water Resources*, 1:5, pp. 251-266, 1978.
21. ASCE Task Committee, Review of Geostatistics in Geohydrology. I: Basic Concepts, *Journal of Hydraulic Engineering*, 116:5, pp. 612-658, 1988.
22. C. V. Deutsch and A. G. Journel, *GSLIB Geostatistical Software Library and User's Guide*. Oxford University Press, New York, 1992.
23. J. D. Dean, P. S. Huyakorn, A. S. Donigian, K. S. Voos, R. W. Schanz, Y. J. Meeks, and R. F. Carsel, *Risk of Unsaturated/Saturated Transport and Transformation of Chemical Concentrations (RUSTIC). Volume 1: Theory and Code Verification*. U.S. Environmental Protection Agency, EPA 600/3-89/048a, Athens, Georgia, 1989.

24. L. Smith, R. A. Freeze, and J. Massmann, Geostatistical Approach to Site Characterization and Risk Assessment Related to Groundwater Contamination at Hazardous Waste Management Sites, in *Risk Assessment for Groundwater Pollution Control*, W. F. McTernan and E. Kaplan (eds.), American Society of Civil Engineers, New York, 1990.

Direct reprint requests to:

William F. McTernan
Professor, School of Civil and Environmental Engineering
Oklahoma State University
Stillwater, OK 74078
e-mail: william.mcternan@okstate.edu